The Plant Cell, Vol. 23: 3654–3670, October 2011, www.plantcell.org

AGAMOUS Terminates Floral Stem Cell Maintenance in *Arabidopsis* by Directly Repressing *WUSCHEL* through Recruitment of Polycomb Group Proteins [W]

Xigang Liu,[a,1] Yun Ju Kim,[a,1] Ralf Müller,[b] Rae Eden Yumul,[a,c] Chunyan Liu,[d] Yanyun Pan,[e] Xiaofeng Cao,[d] Justin Goodrich,[b] and Xuemei Chen[a,2]

[a] Department of Botany and Plant Sciences, Institute of Integrative Genome Biology, University of California, Riverside, California 92521

[b] Institute of Molecular Plant Sciences, University of Edinburgh, Edinburgh EH9 3JH, United Kingdom

[c] ChemGen Integrative Graduate Education and Research Traineeship Program, University of California, Riverside, California 92521

[d] State Key Laboratory of Plant Genomics and National Center for Plant Gene Research, Institute of Genetics and Developmental Biology, Chinese Academy of Sciences, Beijing 100101, China

[e] College of Life Science, Hebei Agricultural University, Baoding 071001, China

Floral stem cells produce a defined number of floral organs before ceasing to be maintained as stem cells. Therefore, floral stem cells offer an ideal model to study the temporal control of stem cell maintenance within a developmental context. AGAMOUS (AG), a MADS domain transcription factor essential for the termination of floral stem cell fate, has long been thought to repress the stem cell maintenance gene *WUSCHEL* (*WUS*) indirectly. Here, we uncover a role of Polycomb Group (PcG) genes in the temporally precise repression of *WUS* expression and termination of floral stem cell fate. We show that AG directly represses *WUS* expression by binding to the *WUS* locus and recruiting, directly or indirectly, PcG that methylates histone H3 Lys-27 at *WUS*. We also show that PcG acts downstream of *AG* and probably in parallel with the known *AG* target *KNUCKLES* to terminate floral stem cell fate. Our studies identify core components of the network governing the temporal program of floral stem cells.

INTRODUCTION

Stem cells possess the potential to generate all or some differentiated cell types during development in a multicellular organism. Certain types of stem cells are active throughout the life of an organism, but others, such as the embryonic stem (ES) cells in animals and the floral stem cells in plants, are precisely terminated, meaning that they cease to function and be maintained as stem cells, in a process that is coordinated with other developmental events. Much is known about the factors that confer stemness in both plants and animals (Mayer et al., 1998; Nichols et al., 1998; Mitsui et al., 2003; Masui et al., 2007), but little is known about how stem cell maintenance is precisely terminated within a developmental context.

Several types of stem cells contribute to the generation of the body plan of a plant. The shoot apical meristem (SAM) harbors stem cells that produce the entire aboveground structures of a plant in an indeterminate manner; these stem cells are active throughout plant development. A floral meristem harbors stem cells that give rise to all organs found in a flower, including sepals, petals, stamens, and carpels. In contrast with the stem cells in the SAM, floral stem cells are determinate insofar as they generate a precise number of floral organs and then cease to be stem cells. The termination of floral stem cell fate is coincident with the development of carpel primordia, the final organs to be made from the floral meristem. However, the termination of floral stem cell maintenance is not simply the differentiation of stem cells into carpel cells because we isolated mutants that uncouple carpel identity specification and the termination of floral stem cell maintenance (Ji et al., 2011; this study). Instead, a mechanism independent of, but coordinated with, organ identity specification is responsible for the precise termination of floral stem cell fate. As such, floral stem cells provide a good model for studying the temporal program of stem cells.

The termination of floral stem cell maintenance involves two key transcription factors, AGAMOUS (AG), a MADS domain protein, and WUSCHEL (WUS), a homeodomain protein. *WUS* is expressed in a few cells known as the organizing center (OC) underneath the floral stem cells and the OC signals to the overlying cells to maintain their stem cell identity (Laux et al., 1996; Mayer et al., 1998). By stage 6 of flower development (stages according to Smyth et al., 1990) when the primordia for the final floral organs

[1] These authors contributed equally to this work.

[2] Address correspondence to xuemei.chen@ucr.edu.

The author responsible for distribution of materials integral to the findings presented in this article in accordance with the policy described in the Instructions for Authors (www.plantcell.org) is: Xuemei Chen (xuemei.chen@ucr.edu).

[W] Online version contains Web-only data.

www.plantcell.org/cgi/doi/10.1105/tpc.111.091538

(carpels) arise, *WUS* expression is shut off, which results in the termination of floral stem cell maintenance. The temporally regulated repression of *WUS* expression requires *AG* (Laux et al., 1996; Lenhard et al., 2001; Lohmann et al., 2001), which also serves as a key factor in specifying the identities of stamens and carpels (Bowman et al., 1989). In an *ag* loss-of-function mutant, stamens are transformed into petals and carpels are replaced by an internal flower to result in a flowers-within-flower phenotype (Bowman et al., 1989). *AG* expression commences at stage 3 in a domain that encompasses that of *WUS* (Drews et al., 1991; Mayer et al., 1998), yet *WUS* expression is not shut off until stage 6. Consequently, *AG* has been considered to be an indirect regulator of *WUS*. In fact, *AG* is known to activate the expression of another transcription factor gene *KNUCKLES* (*KNU*) at stage 6 in a region that encompasses the *WUS*-expressing OC in the floral meristem; *KNU* is in turn necessary for the repression of *WUS* expression (Sun et al., 2009). However, the floral determinacy defects of the *knu-1* mutant are much weaker than those of *ag* null mutants (Bowman et al., 1989; Payne et al., 2004). Although this could be due to the *knu-1* allele not being a null allele, an alternative explanation is that, in addition to activating *KNU* expression, *AG* also represses *WUS* expression through unknown mechanisms.

Polycomb Group (PcG) proteins were first identified as repressors of homeotic genes in *Drosophila melanogaster* (Lewis, 1978; Jürgens, 1985). PcG proteins in *Drosophila* associate in various functionally distinct subcomplexes (reviewed in Müller and Verrijzer, 2009), including Polycomb Repressive Complex2 (PRC2), which trimethylates histone H3 Lys-27 (H3K27) at specific target genes, PRC1, which recognizes the H3K27me3 mark to promote the compaction of chromatin for transcriptional repression, and Pho-Repressive Complex, which is responsible for the recruitment of PcG proteins to genes containing Polycomb response elements. Homologs of all *Drosophila* PRC2 subunit genes are found in *Arabidopsis thaliana* (reviewed in Pien and Grossniklaus, 2007; Köhler and Villar, 2008; Schatlowski et al., 2008; Hennig and Derkacheva, 2009; Zheng and Chen, 2011). In particular, *CURLY LEAF* (*CLF*) and its paralogs *SWINGER* (*SWN*) and *MEDEA* are homologs of *Drosophila E(z)*, the H3K27 methyltransferase. *MEDEA* acts predominantly in the seed, while *CLF* and *SWN* are broadly expressed and act redundantly during vegetative and reproductive development (Goodrich et al., 1997; Grossniklaus et al., 1998; Chanvivattana et al., 2004). *TERMINAL FLOWER2/LIKE HETEROCHROMATIN PROTEIN1* (*TFL2/LHP1*) is considered a functional counterpart of PRC1 because it recognizes, and colocalizes with, H3K27me3 throughout the genome (Turck et al., 2007; Zhang et al., 2007a). *TFL2/LHP1* as the functional PRC1 counterpart is further supported by the similar phenotypes exhibited by *tfl2* mutants and mutants in PRC2 genes (Kotake et al., 2003; Mylne et al., 2006; Sung et al., 2006). No Pho-Repressive Complex homologs or Polycomb response elements have been identified, and how PcG is recruited to specific targets in plants remains largely enigmatic. One recent study showed that a noncoding RNA recruits PRC2 to the *FLC* gene (Heo and Sung, 2011).

In this study, we show that PcG is required for *AG*-mediated repression of *WUS* expression and termination of floral stem cell maintenance. We show that, in addition to indirectly repressing *WUS* expression through the activation of *KNU* expression at stage 6 (Sun et al., 2009), *AG* directly represses *WUS* expression before stage 6 by binding to the *WUS* locus and recruiting PcG to *WUS*. Our studies establish a direct link between *WUS* and *AG*, which has long been known to repress *WUS* expression but is thought to do so indirectly, and establishes a core network of floral stem cell regulators. Furthermore, mutations in two AG binding sites abrogate the termination of *WUS* expression in flower development and reveal the unexpected existence of a group of cells with the unique ability to express *WUS* in mature flowers. This suggests that the earlier *WUS*-expressing OC remains distinct from neighboring cells in mature flowers.

RESULTS

CLF Is Required for the Temporally Regulated Termination of Floral Stem Cell Maintenance

To identify players that regulate the temporal program of floral stem cells, we performed an ethyl methanesulfonate mutagenesis in the *ag-10* background. While *ag* null alleles are defective in both floral stem cell fate termination and floral organ identity specification, as reflected by reproductive-to-perianth organ transformation, as well as a flowers-within-flower phenotype (Bowman et al., 1989), the weak *ag-10* allele is only mildly defective in floral stem cell fate termination and is normal in floral organ identity specification (Ji et al., 2011). *ag-10* flowers generate a full complement of floral organs like the wild type (Figures 1A and 1B), but one to a few siliques on an *ag-10* plant are short and bulged with additional floral organs inside (Figure 1I), reflecting a mild defect in stem cell fate termination. In the *ag-10* mutagenesis screen, mutations that enhanced the mild stem cell defects were isolated based on the presence of bulged siliques throughout the plant.

One such mutant displayed mostly short and bulged siliques (Figures 1D and 1I). Longitudinal sections of stage 7 and older flowers revealed a dome-shaped meristem between the two carpels in this mutant (Figures 1E, 2C, and 2D) but not in the majority of *ag-10* flowers (Figures 1F, 2A, and 2B). In later-staged flowers of this mutant, additional organs were generated inside the primary gynoecia (Figure 1E). Therefore, this recessive mutation enhanced the *ag-10* floral determinacy defect phenotype. Genetic mapping revealed a G-to-A mutation in *CLF*, which resulted in the conversion of amino acid 794 in the SET domain from Arg (R) to His (H) (see Supplemental Figure 1 online). The Arg-794 residue is highly conserved within the SET domain, which is itself conserved in E(z) homologs and is responsible for the H3K27 methyltransferase activity (see Supplemental Figure 1B online). The enhancer mutation was named *clf-47*. The *ag-10 clf-47* double mutant resembled well-characterized *clf* single mutants in that it was dwarfed, exhibited early flowering, and had small and curled leaves (Goodrich et al., 1997). The *clf-47* single mutant did not exhibit obvious defects in floral stem cells (Figures 1C and 1I).

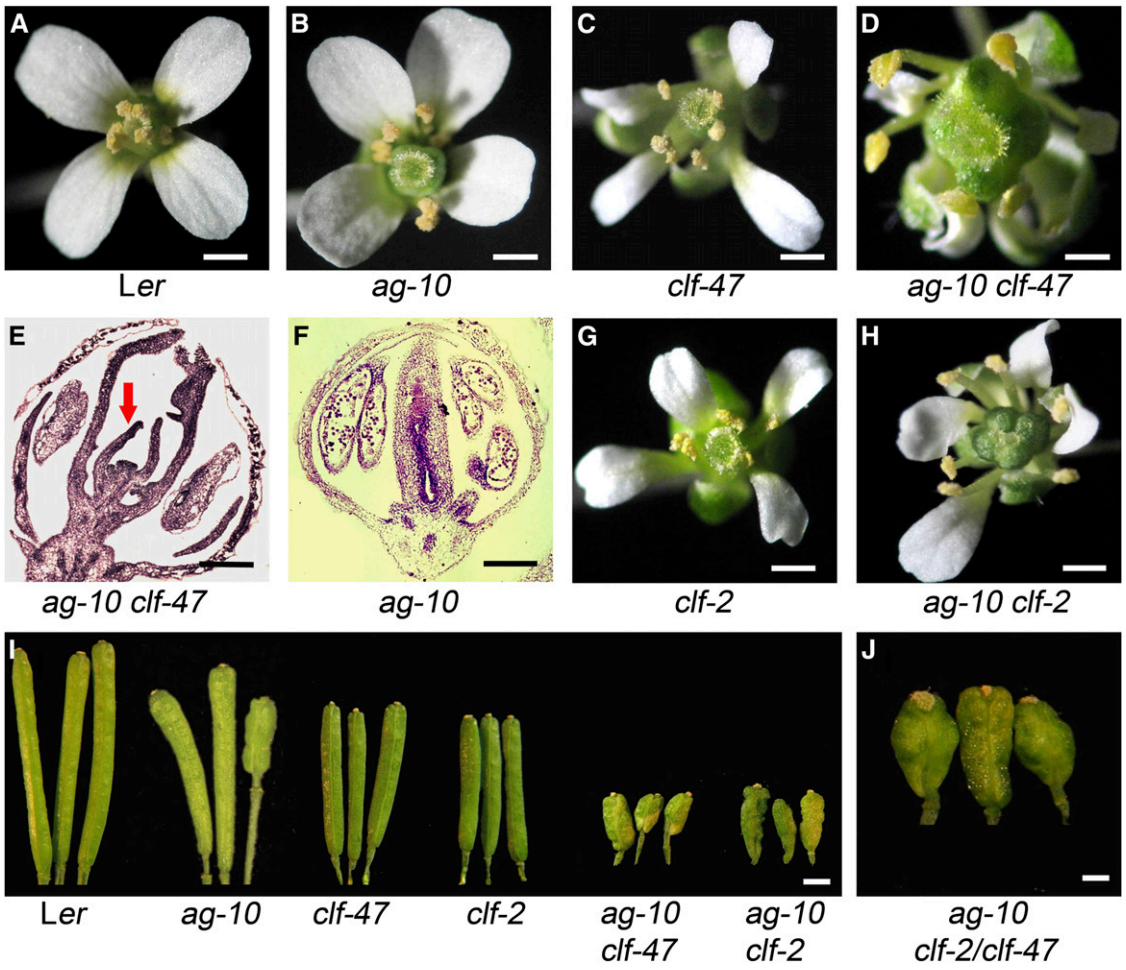

Figure 1. Phenotypes of *ag* and *clf* Single and Double Mutants.

(A) A wild-type (L*er*) flower.
(B) An *ag-10* flower with a slightly enlarged gynoecium.
(C) A *clf-47* flower.
(D) An *ag-10 clf-47* flower with a much more enlarged gynoecium compared with *ag-10*.
(E) and **(F)** Longitudinal sections through stage 11 flowers of *ag-10 clf-47* **(E)** and *ag-10* **(F)** genotypes. In **(E)**, the floral meristem continued to generate organs (arrow) inside the carpels.
(G) A *clf-2* flower.
(H) An *ag-10 clf-2* flower with similar phenotypes to those of *ag-10 clf-47*.
(I) Siliques from plants of the indicated genotypes. Most siliques on an *ag-10* plant were long and thin (represented by the two on the left); one to a few siliques were short and bulged (represented by the one on the right). Most siliques from *ag-10 clf-47* or *ag-10 clf-2* plants were short and bulged.
(J) Siliques from F1 plants of the cross between *ag-10 clf-47* and *ag-10 clf-2*. The siliques were similar in morphology to those of *ag-10 clf-47* or *ag-10 clf-2*.
Bars = 1 mm in **(A)** to **(C)** and **(G)** to **(I)**, 0.75 mm in **(D)**, 0.5 mm in **(J)**, and 100 μm in **(E)** and **(F)**.

To confirm that the floral phenotype of *ag-10 clf-47* was caused by a mutation in *CLF*, we introduced another *clf* allele, *clf-2* (Figure 1G; Goodrich et al., 1997) into *ag-10.* Like *ag-10 clf-47*, the *ag-10 clf-2* double mutant exhibited short and bulged siliques with ectopic floral organs inside (Figures 1H and 1I). In addition, an allelic test was conducted by crossing *ag-10 clf-47* to *ag-10 clf-2*. The resulting F1 plants had both enhanced floral determinacy defects in flowers and vegetative phenotypes characteristic of *clf* mutants (Figure 1J). Collectively, these results show that *CLF* is required for floral meristem determinacy.

CLF Is Necessary for the Temporally Controlled Repression of *WUS* Expression

To investigate the molecular basis of the floral determinacy defects of the *ag-10 clf-47* double mutant, we first performed in situ hybridization to determine the temporal and spatial

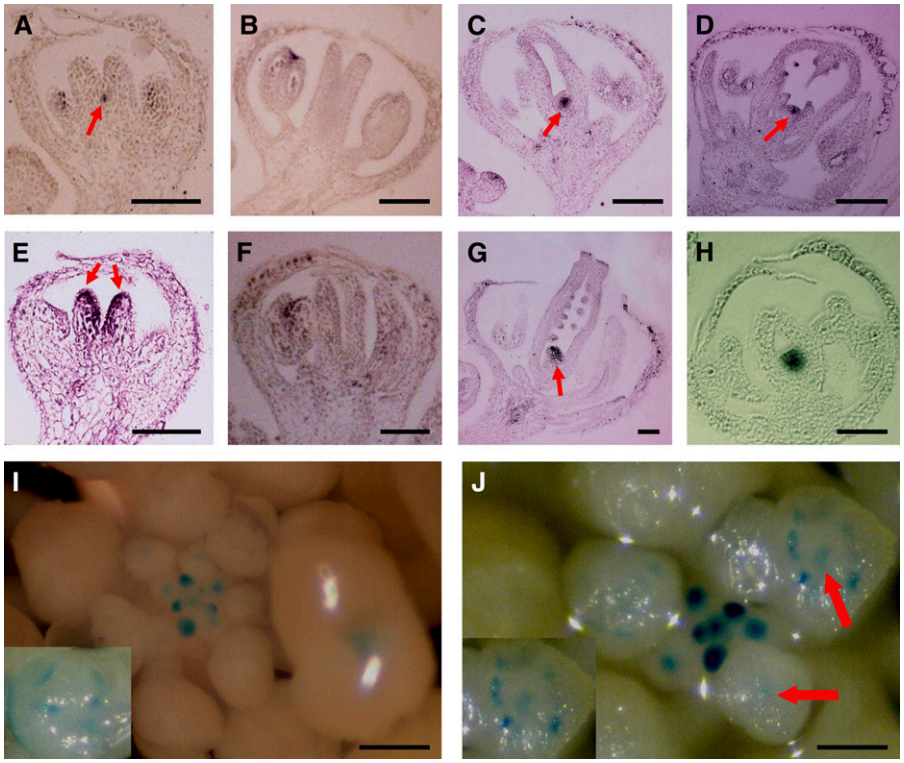

Figure 2. Expression Patterns of *WUS* and *STM* in *ag-10* and *ag-10 clf-47* Flowers.

(A) to **(D)** In situ hybridization with a *WUS* antisense probe. The arrows indicate *WUS* signals.
(A) and **(B)** *WUS* expression was detected in a stage 7 **(A)** but not a stage 9 **(B)** *ag-10* flower.
(C) and **(D)** *WUS* expression was detected in *ag-10 clf-47* flowers at stage 9 **(C)** and stage 11 **(D)**.
(E) to **(G)** In situ hybridization using an *STM* antisense probe. The arrows indicate *STM* signals.
(E) and **(F)** *STM* expression was detected at stage 7 **(E)** but not stage 9 **(F)** in *ag-10* flowers.
(G) *STM* expression was detected in a stage 12 *ag-10 clf-47* flower.
(H) A longitudinal section of a stages 8 or 9 *ag-10 clf-47 pWUS*:*GUS* flower showing GUS staining inside the carpels.
(I) and **(J)** GUS staining in *pWUS*:*GUS* **(I)** and *ag-10 clf-47 pWUS*:*GUS* **(J)** inflorescences. Arrows in **(J)** indicate GUS signals in the center of stages 8 and 9 flowers. The insets are stages 8 and 9 flowers. The ring-like GUS signals were from anthers. The GUS signals inside the ring in **(J)** were from the floral meristem.
Bars = 50 μm in **(A)** to **(H)** and 250 μm in **(I)** and **(J)**.

expression patterns of *WUS*, which promotes stem cell identity, and *STM*, which is required for the acquisition and/or maintenance of meristematic fate (Long et al., 1996), in floral meristems. In the wild type, *WUS* expression is shut off at stage 6 when carpel primordia are formed (Mayer et al., 1998). In the *ag-10* single mutant, stage 7 was the latest stage when *WUS* expression was observed (Figure 2A); only one out of 10 stage 7 flowers examined expressed *WUS*. In the *ag-10 clf-47* double mutant, nine out of 10 stage 7 flowers examined showed *WUS* expression, and the expression persisted in much older flowers (Figures 2C and 2D). Expression in such late-staged flowers was not observed in the *ag-10* single mutant (Figure 2B). Therefore, *CLF* was required for the temporally precise repression of *WUS* expression in the flower. *STM* expression also persisted much longer in the *ag-10 clf-47* double mutant than in the *ag-10* single mutant. In the *ag-10* single mutant, stage 7 was the latest stage when *STM* expression was observed (Figures 2E and 2F); only two out of 10 *ag-10* stage 7 flowers examined showed *STM* expression. Seven out of nine *ag-10 clf-47* flowers had *STM* expression, which persisted in much older flowers (Figure 2G). As *STM* is a marker for meristematic cells, the results suggested that cells retained meristematic activity until a much later stage in *ag-10 clf-47* flowers.

Although our results indicated that *CLF* is required for *WUS* repression in flower development, it was not clear whether *CLF* is involved in the initial repression of *WUS*, which requires *AG*, or in a later step after the initial repression to maintain the repressed state. To monitor *WUS* expression in all floral stages in an inflorescence, we introduced a *pWUS*:*GUS* (for β-glucuronidase) reporter that recapitulates endogenous *WUS* expression patterns (Bäurle and Laux, 2005) into *ag-10 clf-47.* In the wild type, this reporter was active in floral meristems between stages 1 and 6 (Figure 2I). In *ag-10 clf-47*, continuous *GUS* expression was observed from early stages until stages 8 and 9 (Figure 2J). In flowers of stages 8 and 9 when GUS signals were visible in anthers, *GUS* expression was observed in the center of the

flowers in *ag-10 clf-47* but not in the wild type (Figures 2I and 2J, insets). Longitudinal sections of *ag-10 clf-47 pWUS*:*GUS* flowers confirmed prolonged *GUS* expression in late-staged floral meristems (Figure 2H). Importantly, we did not observe any reduction in *GUS* expression at stage 6 in *ag-10 clf-47*. This suggests that *CLF* is required for the initial repression of *WUS*.

To determine whether the prolonged *WUS* or *STM* expression in *ag-10 clf-47* floral meristems underlies the floral determinacy defects, we crossed the loss-of-function *wus-1* mutation (Laux et al., 1996) and the partial loss-of-function *stm-2* mutation (Clark et al., 1996) into *ag-10 clf-47*. The *wus-1* mutation results in premature termination of the floral meristem such that the flower terminates in a central stamen (Figure 3A). *wus-1* was epistatic to *ag-10 clf-47* as *ag-10 clf-47 wus-1* triple mutant flowers also terminated precociously (Figure 3B; see Supplemental Table 1 online). *stm-2* flowers show premature termination of the floral meristem such that they have a reduced number of floral organs (Figure 3C). *stm-2* was also epistatic to *ag-10 clf-47* for floral meristem determinacy (Figure 3D; see Supplemental Table 1 online). These results indicated that the floral

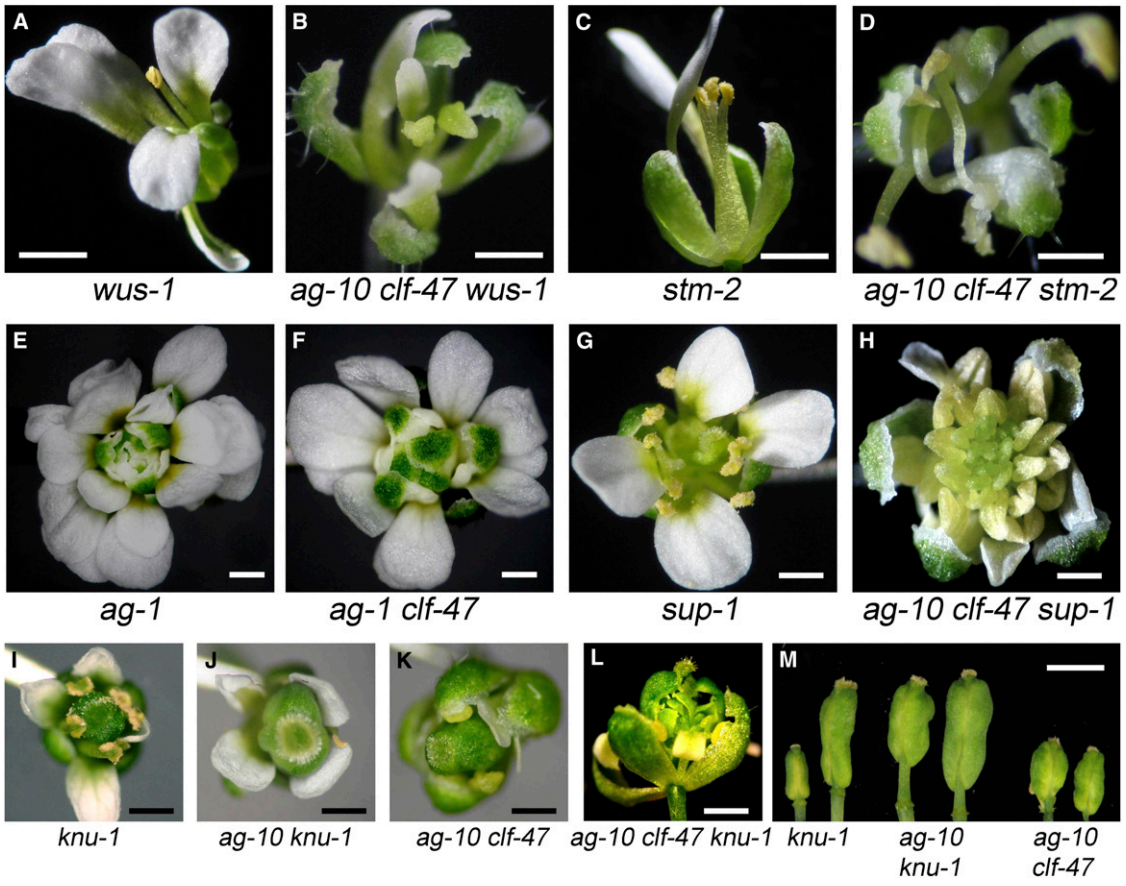

Figure 3. Phenotypes of *clf-47* and *ag-10 clf-47* in Combination with Mutations in Other Floral Meristem Regulators.

(A) A *wus-1* flower that lacked a full complement of floral organs.
(B) An *ag-10 clf-47 wus-1* flower, which was similar to *wus-1* with respect to floral meristem determinacy.
(C) An *stm-2* flower that lacked a full complement of floral organs.
(D) An *ag-10 clf-47 stm-2* flower, which was similar to *stm-2* flowers in terms of floral meristem determinacy.
(E) An *ag-1* flower with a flowers-within-flower phenotype.
(F) An *ag-1 clf-47* flower, which was morphologically identical to *ag-1* flowers.
(G) A *sup-1* flower with more stamens than the wild type.
(H) An *ag-10 clf-47 sup-1* flower, which developed numerous stamens from an indeterminate floral meristem.
(I) A *knu-1* flower.
(J) An *ag-10 knu-1* flower with an enlarged gynoecium.
(K) An *ag-10 clf-47* flower with an enlarged gynoecium.
(L) An *ag-10 clf-47 knu-1* flower with an internal flower replacing the gynoecium.
(M) Siliques from *knu-1*, *ag-10 knu-1*, and *ag-10 clf-47* plants. The *knu-1* silique on the left was a representative silique from young *knu-1* plants, while the one on the right was a representative silique from old *knu-1* plants.
Bars = 1 mm in **(A)** to **(L)** and 2.5 mm in **(M)**.

determinacy defects of *ag-10 clf-47* were due to prolonged *WUS* and *STM* expression.

CLF and *AG* Confer Floral Meristem Determinacy in the Same Genetic Pathway

To determine the genetic relationship between *AG* and *CLF* in the regulation of floral stem cells, we introduced the *clf-47* mutation into the *ag* null mutant *ag-1* background (Bowman et al., 1989). The floral phenotypes of the *ag-1 clf-47* double mutant were identical to those of the *ag-1* single mutant (Figures 3E and 3F), indicating that *CLF* and *AG* act in the same pathway in conferring floral meristem determinacy. Consistent with this finding, both *ag-1* and *ag-10 clf-47* interacted synergistically with *sup-1*, a mutation in *SUPERMAN* (*SUP*), a gene that acts in parallel with *AG* in the regulation of floral stem cells (Bowman et al., 1992). The *sup-1* single mutant flowers exhibit an increased number of stamens and carpels, but the floral meristem eventually terminates in a few carpels (Figure 3G). The *clf-47 sup-1* double mutant flowers had more stamens and carpels than *sup-1* flowers. The *ag-10 clf-47 sup-1* triple mutant exhibited a dramatic enhancement of the floral determinacy defects of both *ag-10 clf-47* and *sup-1* in that they developed numerous stamens following a spiral phyllotaxy from an indeterminate floral meristem (Figure 3H). Similarly, combining *ag-1* with *sup-1* resulted in a drastic enhancement of floral meristem activity (Bowman et al., 1992).

A number of genes are known to promote floral determinacy by maintaining *AG* expression in the center of the floral meristem (Schultz et al., 1991; Alvarez and Smyth, 1999; Carles et al., 2005; Prunet et al., 2008; Das et al., 2009; Maier et al., 2009). To determine whether *CLF* acts similarly, we performed in situ hybridization to examine *AG* expression in wild-type, *ag-10*, and *ag-10 clf-47* flowers. As in the wild type, *AG* transcripts were present in the inner two whorls of *ag-10* and *ag-10 clf-47* floral meristems (see Supplemental Figures 2A to 2F online). Because in situ hybridization is not a quantitative measure of gene expression, we performed immunoblotting to determine the levels of AG protein in wild-type and *ag-10 clf-47* inflorescences and leaves. Consistent with *AG* being a known PcG target (Goodrich et al., 1997), AG protein levels were elevated in *ag-10 clf-47* compared with the wild type in both inflorescences and leaves (see Supplemental Figure 2G online). The fact that *clf-47* resulted in compromised floral determinacy without causing a decrease in *AG* expression suggests that *CLF* is required for *AG*-mediated floral stem cell regulation. This, together with the genetic studies showing that *CLF* and *AG* act in the same pathway, suggests that *CLF* acts downstream of *AG* in terminating floral stem cell maintenance.

Loss of Function in *TFL2/LHP1* Also Enhances *ag-10*

We investigated whether the function of *CLF* in floral meristem determinacy reflects a similar role for PcG. We crossed *tfl2-2* (Larsson et al., 1998), a mutation in the PRC1 component *TFL2/LHP1*, into *ag-10* to determine whether *tfl2-2* also enhances *ag-10*. Since the *tfl2-2* allele is in the Columbia (Col) background, we first crossed it to a line in which the *ag-10* mutation in the Landsberg *erecta* (L*er*) background was introgressed into Col by five backcrosses. Unlike *ag-10* in L*er*, *ag-10*^{Col} did not exhibit any floral determinacy defects (all siliques on a plant were long and thin as in the wild type), indicating that there was a genetic suppressor/modifier in Col. In a *tfl2-2* plant, the rosette leaves are curled and the inflorescence terminates in a few disorganized flowers (Figure 4A; Larsson et al., 1998). The gynoecia in these flowers are thin (Figure 4A), suggesting that the *tfl2-2* mutant itself did not have any floral determinacy defects. The *tfl2-2* mutation enhanced *ag-10*^{Col} in that some gynoecia of *ag-10*^{Col} *tfl2-2* plants consisted of more than two carpels that were partially fused. However, the phenotypes of *ag-10*^{Col} *tfl2-2* were much weaker than those of *ag-10 clf-47*. To determine whether this was due to a suppressor in Col, we crossed *tfl2-2* to *ag-10* in L*er*. In the F2 population, all plants with *tfl2-2* vegetative phenotypes were genotyped for *ag-10*. Among 110 *ag-10 tfl2-2* plants, 32 had severe floral determinacy defects that were similar to, or even more severe than, those of *ag-10 clf-47* plants. The flowers of these *ag-10 tfl2-2* plants had bulged or unfused gynoecia with internal floral organs (Figures 4B and 4D). The remaining *ag-10 tfl2-2* plants had normal siliques (Figure 4C). Since none of the *ag-10 tfl2-2*/*TFL2* or *ag-10 TFL2*/*TFL2* plants had floral determinacy defects, *tfl2-2* was responsible for the loss of floral determinacy in some *ag-10 tfl2-2* plants. The segregation of this phenotype among *ag-10 tfl2-2* plants was consistent with the existence of a single dominant suppressor or several recessive suppressors of *ag-10* in the Col ecotype.

WUS Is a Target of PcG in Flowers and Seedlings

Genome-wide profiling of H3K27me3 with 10-d-old *Arabidopsis* seedlings identified ~4000 genes, including *WUS*, as potential targets of PcG (Zhang et al., 2007b). H3K27me3 was found to be enriched throughout the *WUS* genomic region, including the entire intergenic region between *WUS* and its upstream gene and up to 1.5 kb downstream of the 3′ end of the transcript (Zhang et al., 2007b). To confirm that the H3K27me3 mark at *WUS* was PcG dependent, we performed chromatin immunoprecipitation (ChIP) to examine H3K27me3 levels in wild-type seedlings and in the *clf-28 swn-7* double mutant, which germinates into abnormal seedlings that develop into callus-like tissues (Chanvivattana et al., 2004). H3K27me3 was enriched at the known PcG target *AG* in the wild type, but this enrichment was eliminated in *clf-28 swn-7*, consistent with previous reports (see Supplemental Figure 3 online; Schubert et al., 2006). Similarly, the levels of H3K27me3 at the *WUS* locus were drastically reduced in *clf-28 swn-7* (see Supplemental Figure 3 online). To determine whether *WUS* was a target of PcG in flowers, we performed ChIP to examine H3K27me3 levels at *WUS* in wild-type inflorescences. As in seedlings, H3K27me3 was enriched throughout the *WUS* genomic region in inflorescences (Figure 4F).

Previous studies suggest that PRC1 binds H3K27me3 through TFL2/LHP1 to effect transcriptional inhibition at PcG targets (Turck et al., 2007; Zhang et al., 2007a; Xu and Shen, 2008). Intriguingly, although H3K27me3 was found throughout the *WUS* locus, genome-wide profiling of TFL2/LHP1 occupancy in 10-d-old seedlings revealed that three distinct regions at *WUS* were bound by TFL2/LHP1 (Zhang et al., 2007a). These

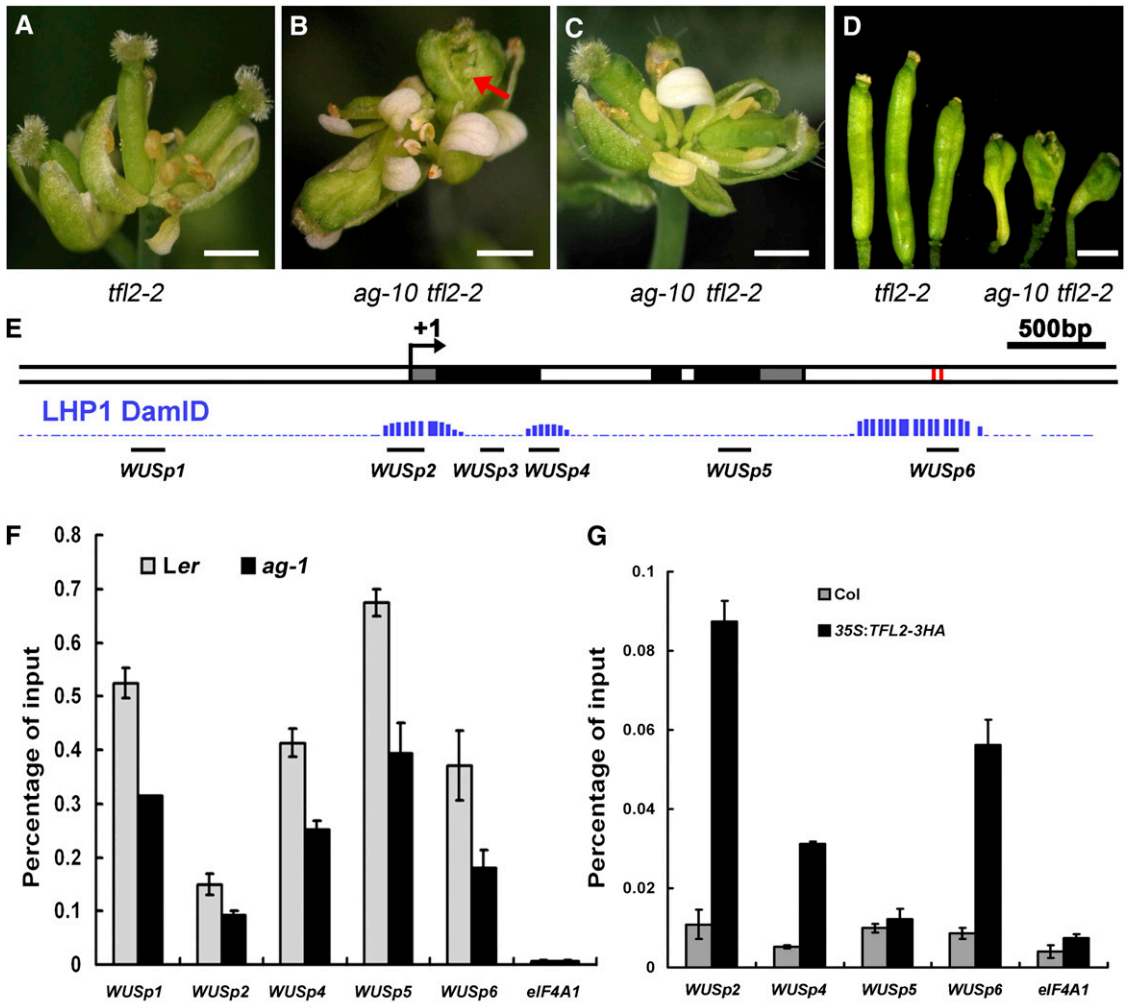

Figure 4. *TFL2/LHP1* Acts in Floral Stem Cell Termination, and *WUS* Is a PcG Target.

(A) A terminal inflorescence composed of several fused flowers in *tfl2-2*. Note that the gynoecia were thin.
(B) A representative inflorescence of *ag-10 tfl2-2* plants with floral determinacy defects. The flowers had bulged gynoecia with ectopic floral organs inside (arrow).
(C) A representative inflorescence of *ag-10 tfl2-2* plants without floral determinacy defects. The gynoecia were thin.
(D) Siliques from plants of the indicated genotypes. The *ag-10 tfl2-2* plants were from the F2 population of the cross between *ag-10* and *tfl2-2*. Only siliques from the *ag-10 tfl2-2* plants with floral determinacy defects are shown. Bars = 1 mm in **(A)** to **(D)**.
(E) A diagram of the *WUS* genomic region with "+1" being the transcription start site. Gray, black, and white rectangles represent 5′ or 3′ untranslated regions, coding regions, and introns or intergenic regions, respectively. The two red rectangles represent the two CArG boxes. The three regions of TFL2/LHP1 occupancy at *WUS* as determined by genome-wide profiling of TFL2/LHP1 binding sites are shown in blue (LHP1 DmID; Zhang et al., 2007a). The regions interrogated for AG, H3K27me3, or TFL2/LHP1 enrichment at *WUS* in this study are shown as black bars.
(F) ChIP with anti-H3K27me3 antibodies to determine the levels of H3K27me3 at *WUS* in wild-type (L*er*) and *ag-1* inflorescences containing stage 8 and younger flowers.
(G) ChIP with anti-HA antibodies in Col (a negative control) and *35S*:*TFL2-3HA* to examine TFL2/LHP1 occupancy at *WUS*. For **(F)** and **(G)**, the regions examined are diagramed in **(E)**. *eIF4A1* served as a negative control. Error bars represent SD, which were calculated from three technical repeats. Three biological replicates gave similar results.

were *WUSp2* at the transcription start site, *WUSp4* in the first intron, and *WUSp6* located ~800 bp downstream of the coding region (Figure 4E). We determined whether TFL2/LHP1 was associated with the *WUS* locus at these regions in inflorescences by ChIP with anti-HA antibodies in *35S*:*TFL2-3HA* (Liu et al., 2009). We found that TFL2/LHP1 was indeed enriched at these three specific regions but not at another region (*WUSp5*) tested at the *WUS* locus (Figure 4G). The enrichment of both H3K27me3 and TLF2/LHP1 at *WUS* in inflorescences suggests that *WUS* is a target of PcG in flowers.

AG Binds the *WUS* Locus in Vivo and Directly Represses *WUS* Expression

The restricted distribution of TFL2/LHP1 relative to that of H3K27me3 at *WUS* indicates that the H3K27me3 mark alone is not sufficient for TFL2/LHP1 recruitment to targets. Given that *AG* is a major factor in repressing *WUS* expression, we hypothesized that *AG* contributes to the recruitment of TFL2/LHP1 to *WUS*. This hypothesis would only be possible if AG binds the *WUS* locus in vivo. We decided to test this hypothesis despite previous assumptions that *AG* represses *WUS* expression indirectly. AG occupancy at multiple positions along the *WUS* locus was examined by ChIP using anti-AG antibodies in wild-type inflorescences. The *ag-1* null mutant, from which no AG protein was detectable by immunoblotting with the antibodies, served as a negative control. Among six sites spanning the *WUS* locus from −1367 to +2702 (+1 being the transcription start site) examined, enrichment of AG at two specific sites at *WUS* was found (Figure 5A). Intriguingly, the AG binding sites overlapped with two of the three TFL2/LHP1 binding sites, *WUSp2* and *WUSp6* (Figures 4G and 5A).

The in vivo binding of AG to *WUS* prompted us to determine whether *AG* directly represses *WUS* expression. We took advantage of the established *35S:AG-GR ag-1* line in which the functional AG-glucocorticoid receptor (GR) fusion protein could be activated by dexamethasone (DEX) (Gómez-Mena et al., 2005; Sun et al., 2009). We treated *35S:AG-GR ag-1* inflorescences with either DMSO (control) or DEX, and at 2 h after treatment, collected inflorescences containing stage 8 and younger flowers (to enrich for tissues with *WUS* expression) and examined *WUS* expression by quantitative real-time RT-PCR. A small but consistent and statistically significant decrease in *WUS* expression was observed upon DEX treatment (Figure 5B). Next, to determine whether this repression was direct, we performed the DMSO and DEX treatments in the presence of the protein synthesis inhibitor cycloheximide (CHX). *WUS* expression was also reduced in CHX/DEX-treated samples relative to the CHX-treated control samples (Figure 5B). This indicates that *AG* was able to directly repress *WUS* expression. We were aware that a previous study using *35S:AG-GR ag-1* inflorescences containing flower buds of stages 1 to 10 showed that AG induction activated *WUS* expression at 8 h postinduction (Ito et al., 2004). To reconcile these results, we monitored *WUS* expression in a postinduction time course (0 to 24 h). Consistent with the previous study as well as our results above, we found a reduction in *WUS* expression in early time points but an increase in *WUS* expression at 12 and 24 h (see Supplemental Figure 4A online). This increase in *WUS* expression in later time points probably reflected a role of *AG* in the activation of *WUS* expression in anthers and carpels. The expected changes in the expression of *APETALA1* and *SPOROCYTELESS*, two known *AG* targets (Ito et al., 2004), showed that AG activity was being effectively activated by our treatments (see Supplemental Figures 4B and 4C online).

An AG Binding Site Is Necessary for *WUS* Repression

MADS domain–containing proteins, including AG, bind a distinct DNA motif called the CArG box with $CC(A/T)_6GG$ as the consensus sequence (Huang et al., 1993; Shiraishi et al., 1993). AG has been shown to bind to the consensus sequence and variants with one to a few nucleotide changes (Huang et al., 1993; Shiraishi et al., 1993; Riechmann et al., 1996; Sun et al., 2009). We inspected the *WUSp2* and *WUSp6* regions (Figure 4E) that were bound by AG and TFL2/LHP1 in vivo for potential CArG boxes with no more than a single nucleotide difference from the consensus sequence. While we did not identify any CArG boxes in the *WUSp2* region, two tandem sequences resembling CArG

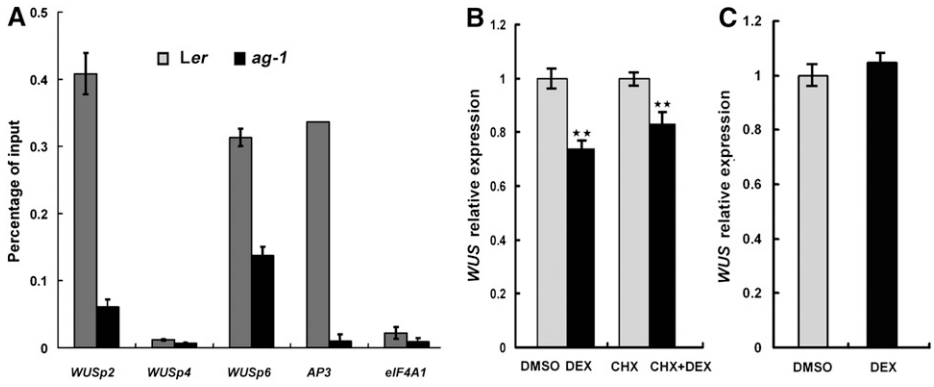

Figure 5. AG Binds the *WUS* locus and Represses *WUS* Expression Directly.

(A) ChIP using anti-AG antibodies to determine AG occupancy at *WUS*. The null allele *ag-1* and the *eIF4A1* locus both served as negative controls. *AP3*, a known direct target of *AG* (Gómez-Mena et al., 2005), served as a positive control.

(B) Real-time RT-PCR to determine *WUS* transcript levels in *35S:AG-GR ag-1* inflorescences containing stage 8 and younger flowers. Inflorescences were treated with DMSO, DEX, CHX, or CHX plus DEX. Two hours later, the inflorescences were dissected to remove old flowers and harvested for RNA extraction and RT-PCR. Four biological replicates were performed for the DMSO/DEX experiment, and five were performed for the CHX/DEX experiment. Error bars represent SD, which were calculated from these biological repeats. The calculated P values for both experiments were 0.011.

(C) Real-time RT-PCR to measure *WUS* transcript levels in *35S:AG-GR ag-1 clf-47* inflorescences. Chemical treatments and RNA isolation were as in **(B)**.

boxes were found in the *WUSp6* region (Figure 6A) in Col. A single nucleotide change in each CArG box was found in the L*er* sequence, but at least one CArG box remained intact in L*er* (Figure 6A).

We employed a reporter gene approach to determine whether the CArG boxes are necessary for the repression of *WUS* in flower development. We generated *WUS1.6*:*GUS*:*WUS3′wt*, in which *GUS* replaced the *WUS* coding sequence in the *WUS* genomic region (−1658 to +2943; position 1 being the transcription start site as in Bäurle and Laux, 2005), and *WUS1.6*:*GUS*:*WUS3′mut*, in which the two CArG boxes were mutated (Figure 6A). None of the 43 transgenic plants carrying the wild-type transgene showed any GUS staining in inflorescences (Figure 6B), consistent with previous findings (Bäurle and Laux, 2005). By contrast, all 34 transgenic plants containing the mutant transgene showed strong GUS signals in both the inflorescence meristem and floral meristems (Figure 6C). Longitudinal sections revealed GUS signals in the inflorescence meristem and young floral meristems not only in the rib zone in which *WUS* is expressed but also in the central zone containing the stem cells (Figure 6F; see Supplemental Figures 5A and 5B online). The expanded GUS-positive domain was not due to the spread of the GUS product to neighboring cells since in situ hybridization using a *GUS* antisense probe also detected the presence of *GUS* mRNA in the central zone of inflorescence and floral meristems (see Supplemental Figures 5C and 5D online). More importantly, GUS signals were present in a small number of cells throughout flower development, including in late-staged flowers with well-developed gynoecia (Figure 6G). These results indicate that the CArG boxes are necessary for the repression of *WUS* expression both spatially and temporally. Since *AG* is not expressed in the inflorescence meristem, the expression of the mutant reporter transgene in the inflorescence meristem suggests that AG cannot be the only MADS domain protein repressing *WUS* expression through the two CArG boxes.

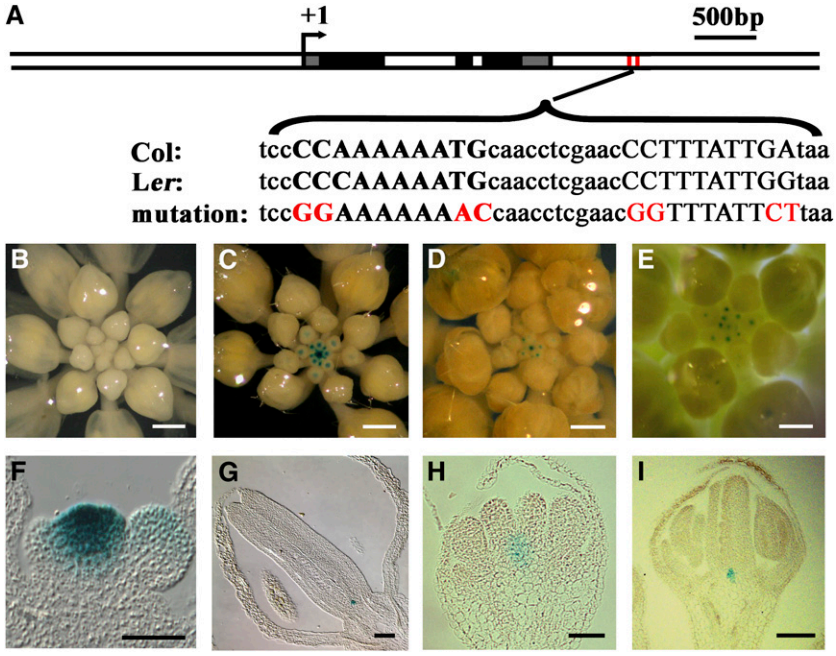

Figure 6. Two CArG Boxes within the AG and TFL2/LHP1 Binding Sites at *WUS* Are Required for the Repression of *WUS* Expression throughout Flower Development.

(A) A diagram of the *WUS* genomic region as in Figure 4E. The sequences of the region containing the two CArG boxes (capital letters) from Col and L*er* as well as the mutated versions are shown. A typical CArG box is $CC(A/T)_6GG$, but slight variants also serve as functional CArG boxes.
(B) A representative inflorescence of *WUS1.6*:*GUS*:*WUS3′wt* transgenic plants showing no GUS staining.
(C) A representative inflorescence of *WUS1.6*:*GUS*:*WUS3′mut* transgenic plants showing strong GUS staining in the inflorescence meristem and floral meristems.
(D) An inflorescence of a *WUS3.2*:*GUS*:*WUS3′wt* transgenic plant showing GUS staining in the inflorescence meristem and young floral meristems.
(E) An inflorescence of a *WUS3.2*:*GUS*:*WUS3′mut* transgenic plant with GUS signals in apparently older flowers than in **(D)**.
(F) and **(G)** Longitudinal sections of an inflorescence **(F)** or a stage 14 flower **(G)** of *WUS1.6*:*GUS*:*WUS3′mut* transgenic plants. In **(F)**, the inflorescence meristem (center) is flanked by a stage 1 and a stage 2 floral primordia. GUS signals were present in the inflorescence meristem. In **(G)**, GUS signals were present at the base of the gynoecium.
(H) A longitudinal section of a stage 7 *WUS3.2*:*GUS*:*WUS3′wt* flower. This was the latest stage when *GUS* expression could be detected in this genotype.
(I) A longitudinal section of a stage 12 flower from *WUS3.2*:*GUS*:*WUS3′mut* transgenic plants. *GUS* expression was detected at the base of the gynoecium.
Bars = 250 μm in **(B)**, **(D)**, and **(E)**, 400 μm in **(C)**, and 50 μm in **(F)** to **(I)**.

We also sought to evaluate the role of the CArG boxes in the context of the 3.2-kb *WUS* promoter, which was found to be sufficient to drive reporter gene expression in patterns reminiscent of *WUS* (Bäurle and Laux, 2005). We generated *WUS3.2*:*GUS*:*WUS3′wt* and *WUS3.2*:*GUS*:*WUS3′mut* plants containing a 3.2-kb promoter region. Indeed, plants carrying the wild-type transgene showed *GUS* expression in the inflorescence meristem and young floral meristems as previously reported (Figure 6D; Bäurle and Laux, 2005). Plants carrying the mutant transgene showed *GUS* expression not only in the inflorescence meristem and young floral meristems but also in later-staged flowers than those carrying the wild-type transgene (cf. Figures 6D and 6E). This was confirmed by examination of GUS signals in sections of flowers of various stages. While the latest stage when GUS signals were visible for *WUS3.2*:*GUS*:*WUS3′wt* flowers was stage 7 (Figure 6H), GUS staining was evident in a small number of cells at the base of the gynoecia in stage 12 *WUS3.2*:*GUS*:*WUS3′mut* flowers (Figure 6I).

AG Recruits PcG to *WUS* to Repress *WUS* Expression

Having shown that AG binds to the *WUS* locus in vivo and that the binding sites are crucial for the termination of *WUS* expression in flower development, we proceeded to test the hypothesis that *AG* is required for the recruitment of PcG to *WUS*. We first examined whether the *ag-1* mutation led to a change in H3K27me3 levels and TFL2 occupancy at *WUS*. ChIP with inflorescences containing flower buds of stages 1 to 8 (older flowers were removed to enrich for meristematic cells) showed that H3K27me3 levels throughout the *WUS* locus were reduced in *ag-1* compared with L*er* (Figure 4F). ChIP was performed to examine TFL2/LHP1 occupancy at *WUS* in *35S*:*TFL2-3HA* versus *35S*:*TFL2-3HA ag-1* inflorescences containing stage 8 and younger flowers. TFL2/LHP1 occupancy at *WUS* was drastically decreased in *ag-1* at *WUSp2* and *WUSp6*, regions bound by AG, but not at *WUSp4*, a region not bound by AG (Figure 7A). These results were consistent with, but not sufficient to support, the conclusion that AG recruits PcG to *WUS* because the reduction in H3K37me3 levels and TFL2/LHP1 occupancy could be a consequence of prolonged *WUS* expression in *ag-1*. To confirm a role of *AG* in PcG recruitment to *WUS*, we took advantage of the *35S:AG-GR ag-1* system and examined the levels of H3K27me3 at *WUS* upon AG induction. H3K27me3 levels were increased throughout the *WUS* locus at 2 h after AG induction (Figure 7B), suggesting that AG plays an active role in recruiting PcG to *WUS*.

These findings raised the possibility that *AG* represses *WUS* expression through the repressive activities of PcG. We took advantage of the *35S*:*AG-GR ag-1* system, with which we had shown that *WUS* transcript levels were detectably reduced at 2 h following DEX treatments, to test this possibility. We first crossed *35S*:*AG-GR ag-1* with *clf-47* to produce *35S*:*AG-GR ag-1 clf-47* plants. These plants were then treated with DEX or the DMSO control, and *WUS* transcript levels were assayed by real-time RT-PCR at 2 h following the chemical treatments. A consistent decrease in *WUS* transcript levels was observed in *35S*:*AG-GR ag-1* (Figure 5B), but no changes in *WUS* transcript levels were detected in *35S*:*AG-GR ag-1 clf-47* (Figure 5C), indicating that *AG*-mediated repression of *WUS* expression requires PcG.

AG Has a Direct and an Indirect Role in the Repression of *WUS* Expression

AG is known to indirectly repress *WUS* expression through the activation of *KNU* expression (Sun et al., 2009). Our results indicate that *AG* also has a direct role in the termination of floral stem cell maintenance by repressing *WUS* expression through the recruitment of PcG. If these were independent functions of *AG*, we would expect *clf* and *knu* mutations to exhibit additive genetic interactions. Thus, we examined the genetic relationship between *KNU* and *CLF*. First, we crossed *knu-1*, which

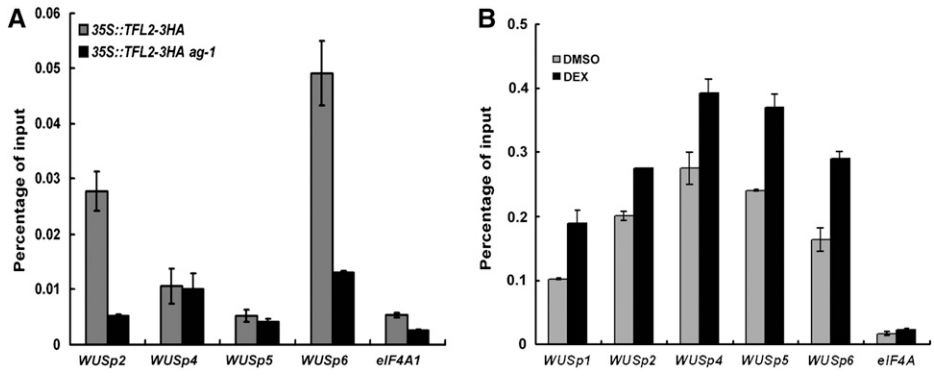

Figure 7. *AG* Recruits PcG to *WUS*.

(A) ChIP using anti-HA antibodies to determine TFL2/LHP1 occupancy at *WUS* in *35S*:*TFL2-3HA* and *35S*:*TFL2-3HA ag-1* inflorescences.
(B) ChIP using anti-H3K27me3 antibodies in DMSO- or DEX-treated *35S*:*AG-GR ag-1* inflorescences. At 2 h after treatments, inflorescences were dissected to remove stage 9 and older flowers and used for ChIP. In **(A)** and **(B)**, real-time PCR reactions were performed with immunoprecipitated and total input DNA. Error bars represent SD, which were calculated from three technical repeats. Three biological replicates gave similar results. The regions interrogated are as diagramed in Figure 4E. *eIF4A1* served as a negative control.

was isolated in the Wassilewskija background (Payne et al., 2004) but was crossed into Landsberg once, into *ag-10*. The gynoecia of *knu-1* plants were initially short and thin, but some were bulged in late-staged plants consistent with the development of an ectopic gynoecium inside the primary gynoecia (Figures 3I and 3M; Payne et al., 2004). The *ag-10 knu-1* double mutant exhibited bulged gynoecia throughout the plant and in younger plants compared with the *knu-1* single mutant (Figures 3J and 3M), suggesting that *knu-1* enhanced the *ag-10* floral determinacy defects. Next, we generated the *ag-10 clf-47 knu-1* triple mutant. Flowers of the triple mutant had much more severe floral determinacy defects than either *ag-10 knu-1* or *ag-10 clf-47* in that the gynoecia were replaced by a new flower (cf. Figures 3L and 3M). The enhancement of *knu-1* by *clf-47* suggests that *KNU* and *CLF* act in parallel in the control of floral determinacy and is consistent with our model that *AG* confers floral determinacy through two mechanisms: the direct repression of *WUS* expression through PcG recruitment to *WUS* and indirect repression of *WUS* expression through the activation of *KNU* expression. However, the fact that *knu-1* may not be a null allele and that *CLF* has a paralog with partially redundant functions complicates the genetic interpretations.

Next, we sought to validate the two independent functions of *AG* with temporal resolution. The activation of *KNU* expression occurs at stage 6 in flower development and coincides with the termination of *WUS* expression (Payne et al., 2004; Sun et al., 2009). However, *AG* expression commences at stage 3, and our results show that *AG* can recruit PcG to directly repress *WUS* expression. This raises the question of when *AG* starts to repress *WUS* expression in flower development. Intriguingly, it was noted that in situ hybridization analysis appeared to show that *WUS* expression was highest at stages 2 and 3 (Lenhard et al., 2001), suggesting that *WUS* expression began to decline at stages 3 and 4. To quantify *WUS* expression in flower development and to determine when *AG* starts to repress *WUS* expression, we performed laser capture microdissection of floral meristems at various stages followed by real-time RT-PCR in wild-type and *ag-1* inflorescences. A circular area identical in size at the center of stages 1 and 2, 3, 4 and 5, or 6 floral meristems was captured from serial sections to ensure that all cells corresponding to a particular meristem zone were collected from a floral meristem (see Supplemental Figure 6 online for an example of the dissected areas). Consistent with prior in situ hybridization results (Drews et al., 1991; Mayer et al., 1998), *WUS* expression was terminated by stage 6 and *AG* expression commenced at stage 3 (Figures 8A, 8B, and 8D), suggesting that our laser capture of the floral meristems was precise. In the wild type, *WUS* expression peaked at stage 3 and decreased by 20% at stages 4 and 5 (Figure 8A). The small decrease in stages 4 and 5 was

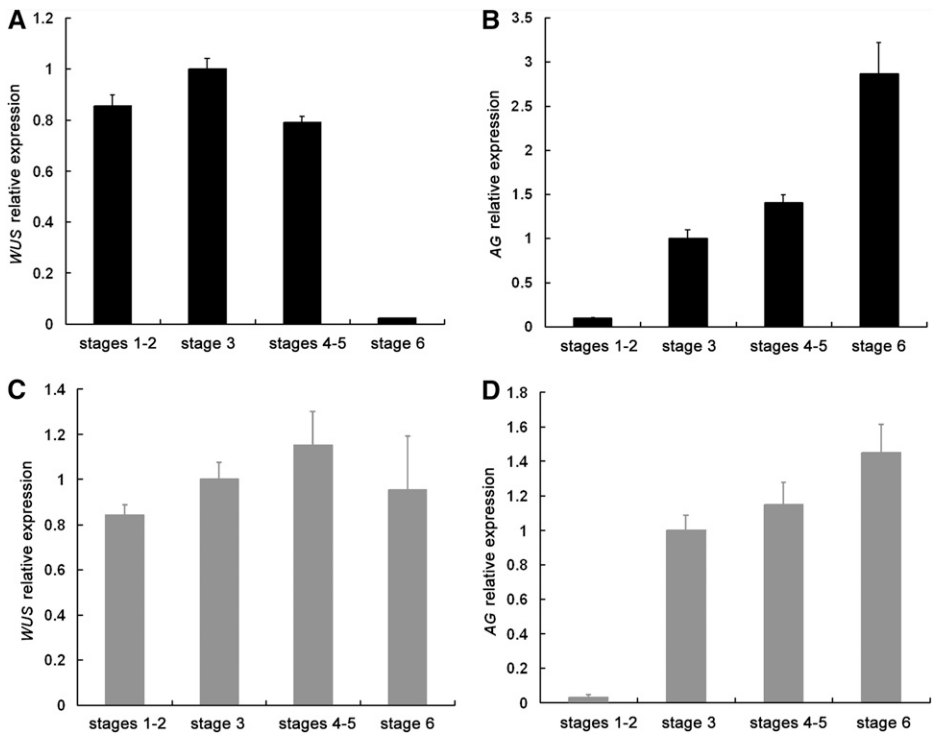

Figure 8. Quantitative Measurements of *WUS* and *AG* Expression at Various Stages in Flower Development.

Laser capture microdissection was performed to collect cells from the central region of a floral meristem of a defined stage in the wild type (**[A]** and **[B]**) and *ag-1* (**[C]** and **[D]**). Real-time RT-PCR was then performed to examine the levels of *WUS* (**[A]** and **[C]**) and *AG* (**[B]** and **[D]**) transcripts using *UBQ5* as the internal control. The levels of expression were shown as relative to those of stage 3, which were set to 1.0. Error bars represent SD, which were calculated from three technical repeats. Two biological replicates gave nearly identical results.

reproducible in two biological replicates and, more importantly, absent in *ag-1* flowers (Figure 8C), suggesting that *AG* represses *WUS* expression starting at stages 4 and 5. Taken together, we propose that *AG* starts to repress *WUS* expression soon after *AG* expression begins by recruiting PcG to *WUS*. This direct effect probably occurs from stages 4 to 6, but the indirect effect through *KNU* occurs at stage 6, and together the two mechanisms result in the termination of *WUS* expression (Figure 9).

DISCUSSION

Stem Cell Termination in Plants and Animals Employs a Conserved Mechanism

PcG proteins repress the expression of a multitude of genes in a developmentally regulated manner in both plants and animals. Studies in animal ES cells show that PcG is required for the differentiation of ES cells into other cell types and that key ES cell maintenance genes are targets of PcG (Boyer et al., 2006; Pasini et al., 2007; Shen et al., 2008). Our studies show that the plant PcG is required for the temporally regulated termination of floral stem cell fate by repressing the expression of the stem cell maintenance gene *WUS*. Therefore, both plants and animals use PcG to regulate stem cell maintenance.

The Fate of the *WUS*-Expressing OC Cells in the Floral Meristem

The *WUS*-expressing cells in the SAM and floral meristems constitute the OC that communicates to the overlying cells to specify their stem cell identity. In floral meristems, the OC, as marked by *WUS* expression, is present from stages 1 to 6. What happens to the OC cells after stage 6? Presumably, the OC cells are incorporated into carpels; they become assimilated and are no different from surrounding carpel cells. An unexpected finding from this study is that the OC cells probably retain their uniqueness even after the cessation of *WUS* expression. Our data reveal that the expression of the *GUS* reporter gene continues in a group of cells at the base of the carpels in late-staged *WUS1.6*:*GUS*:*WUS3′mut* and *WUS3.2*:*GUS*:*WUS3′mut* flowers (Figures 6G and 6I), thus revealing the presence of a group of cells at the base of carpels that is molecularly distinguishable from surrounding cells. Since these cells are likely descendants of earlier *WUS*-expressing OC cells, it is likely that OC cells remain distinct from surrounding carpel cells in late-staged flowers. This, together with the genetic uncoupling of carpel identity specification and stem cell maintenance in *ag-10*, *ag-10 ago10* (Ji et al., 2011), and *ag-10 clf-47*, reinforces the conclusion that stem cell termination is not simply the differentiation of stem cells or OC cells into carpel cells.

AG Acts in Floral Stem Cell Termination via Two Mechanisms

As a key temporal regulator of floral stem cells, *AG* has been thought to terminate floral stem cell maintenance by indirectly repressing *WUS* expression. In this study, we show that AG binds two CArG boxes ~1 kb downstream of the *WUS* coding region and that these CArG boxes are crucial in the repression of *WUS* expression. We also show that induction of AG-GR results in the repression of *WUS* expression in the absence of protein synthesis, suggesting that AG is a direct repressor of *WUS*. Therefore, we propose that *AG* achieves the temporally precise repression of *WUS* expression through two parallel mechanisms: the transcriptional activation of *KNU*, which in turn acts to repress *WUS*, and the direct repression of *WUS* through the recruitment of PcG to *WUS* (Figure 9). In addition, our laser capture microdissection experiments show that *AG* starts to repress *WUS* expression at stages 4 and 5. It is likely *AG* acts directly on *WUS* in stages 4 to 6 and exerts its indirect effects on *WUS* repression through *KNU* at stage 6 (Figure 9).

A previous study showed that the 5′ regulatory region of *WUS* between −595 and −99 (+1 being the transcription start site), when provided in four copies, was sufficient to confer the correct spatial and temporal patterns of *WUS* expression to *GUS* (Bäurle and Laux, 2005). Our work shows that the CArG boxes in the 3′ region have strong influences on *WUS* expression and implicates MADS domain proteins in addition to AG that bind the two CArG boxes in vivo. These findings do not contradict each other because transcriptional regulatory regions usually consist of multiple positive and negative elements that exert additive or combinatorial effects on gene expression.

Recruitment of PcG to *WUS* Requires *AG*

How PcG is recruited to specific loci is a major outstanding question in both mammals and plants. In this study, we found that the MADS domain transcription factor AG binds two of the

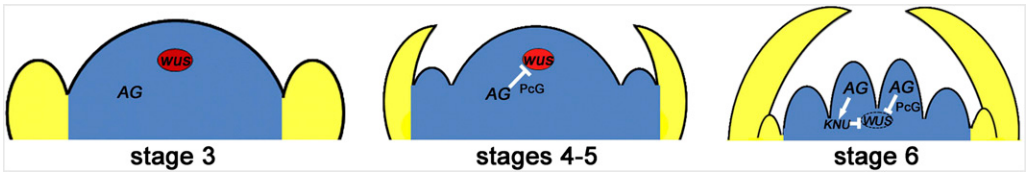

Figure 9. A Model of the Termination of Floral Stem Cell.

AG terminates floral stem cell maintenance by repressing *WUS* expression (Lenhard et al., 2001; Lohmann et al., 2001). A previous study (Sun et al., 2009) showed that *AG* represses *WUS* expression indirectly by activating *KNU*, which in turn represses *WUS* expression directly or indirectly. Data presented in this study show that *AG* also directly represses *WUS* expression by recruiting PcG to *WUS*. Genetic studies are consistent with *KNU* and PcG acting downstream of *AG* and in parallel to each other in terminating floral stem cell maintenance.

three regions that are also bound by TFL2/LHP1 at the *WUS* locus. The specific reduction in TFL2/LHP1 occupancy at these two regions (but not at the third region) in *ag-1* suggests that AG promotes the recruitment of TFL2/LHP1 to *WUS*. A previous study found that another MADS domain protein, SHORT VEGETATIVE PHASE, promotes the recruitment of TFL2/LHP1 to the *SEP3* gene (Liu et al., 2009). Therefore, transcription factors may play a general role in PcG recruitment to targets in plants. How AG recruits TFL2/LHP1 or PRC2 to *WUS* is currently unknown. Extensive coimmunoprecipitation studies between AG and TFL2/LHP1 or AG and CLF failed to detect any association between the proteins in vivo. However, it cannot be ruled out that AG recruits PcG to *WUS* through protein–protein interactions because the coimmunoprecipitation experiments were limited in sensitivity because the OC in which the interactions would take place constituted a small portion of the tissues examined. Alternatively, AG may promote the production of noncoding transcripts, which in turn serve to recruit either PRC2 or TFL2/LHP1. Increasing evidence points to the involvement of noncoding RNAs in PcG recruitment to targets in animals and plants (Rinn et al., 2007; Zhao et al., 2008; Khalil et al., 2009; Kanhere et al., 2010; Tsai et al., 2010; Yap et al., 2010; Heo and Sung, 2011).

METHODS

Plant Materials

All mutants or transgenic lines are in the L*er* background with the exception of *tfl2-2* (Larsson et al., 1998) and *35S*:*TFL2-3HA* (Sun et al., 2009), which are in the Col background; *knu-1* (Payne et al., 2004), which was isolated in the Wassilewskija background but was crossed once into L*er*; and *ag-10*^{col}, in which *ag-10* in L*er* was introgressed into Col through five backcrosses. *Arabidopsis thaliana* plants were grown at 23°C under continuous light. The *clf-47* allele described in this study is an independent isolate (in Landsberg) of the *clf-81* mutation described by Schubert et al. (2006) and isolated in the Col-0 background by H. Tsukaya.

Ethyl Methanesulfonate Mutagenesis

ag-10 seeds (1 mL, ~1000 seeds/100 μL) were washed with 0.1% Tween 20 for 15 min, incubated with 0.2% ethyl methanesulfonate for 12 h, and washed three times with 10 mL water each (1 h for each wash on a rotator). *ag-10* enhancers were isolated in the M2 generation based the presence of bulged siliques throughout the plant. The mutants were backcrossed at least two times to *ag-10* before further studies.

Map-Based Cloning of *CLF*

ag-10 clf-47 (L*er*) was crossed to *ag-10*^{col}. In the F2 population, plants showing the *ag-10 clf-47* phenotypes were selected as the mapping population. Initially, 27 *ag-10 clf-47* plants were used for rough mapping, which showed that *clf-47* was linked to the marker nga1126 on chromosome 2. For fine mapping, we designed new simple sequence length polymorphic or cleaved-amplified polymorphic sequence markers in this region according to polymorphisms between L*er* and Col from the Monsanto Arabidopsis Polymorphism and Ler Sequence database (http://www.Arabidopsis.org/Cereon). *clf-47* was mapped to a 150-kb region covered by the BACs T16B14 and F3N11. The *CLF* gene was identified as a candidate gene and sequenced from the mutant.

Generation of Mutant Combinations

To generate double or triple mutants involving *ag-10* or *ag-10 clf-47*, the *ag-10 clf-47* double mutant was crossed to *sup-1* (Bowman et al., 1992), *stm-2*/+ (Clark et al., 1996), *ag-1*/+ (Bowman et al., 1989), and *wus-1*/+ (Laux et al., 1996). In the F2 generation, plants resembling *clf* mutants in vegetative phenotypes were screened for floral phenotypes characteristic of *sup-1*, *stm-2*, *ag-1*, and *wus-1* flowers. Then, plants with wild-type and *ag-10/ag-10* genotypes at the *AG* locus were identified by molecular genotyping. To generate *ag-10 clf-47 knu-1*, *ag-10 knu-1*, and *clf-47 knu-1*, *ag-10 clf-47* plants were crossed to *knu-1*. In the F2 population, all three mutations were genotyped to identify plants of the correct genotypes.

For *ag-10* genotyping, PCR was performed on genomic DNA using primers *JAGp75* and *JAGp76* (see Supplemental Table 2 online), and the PCR products were digested by *Bst*XI. The *ag-10* mutation abolishes this restriction site. For *clf-47* genotyping, PCR products amplified from genomic DNA using primers *CLFmuF* and *CLFmuR* (see Supplemental Table 2 online) were subjected to *Bstu*I digestion. The *clf-47* mutation abolishes the restriction site. For *knu-1* genotyping, PCR was performed on genomic DNA with the primers *knu-1genoF* and *knu-1genoR* (see Supplemental Table 2 online), and the PCR products were digested with *HpyCH4*III. *knu-1* abolishes this restriction site.

Plasmid Construction

To construct *WUS1.6*:*GUS*:*WUS3′wt*, PCR was performed with the primers *WUSGUSF* and *WUSGUSR* (see Supplemental Table 2 online) using genomic DNA from *pWUS*:*GUS* plants (Bäurle and Laux, 2005) as the template. Since both the endogenous *WUS* locus and the transgene could be amplified, the PCR products were digested with *Eco*RV to eliminate the *WUS* genomic DNA, and the remaining PCR products corresponding to the transgene were cloned into *pENTR/D-TOPO* (Invitrogen). Sequencing was conducted to ensure the integrity of the clone. To construct *WUS1.6*:*GUS*:*WUS3′mut*, site-directed mutagenesis was conducted on the *WUS1.6*:*GUS*:*WUS3′wt* plasmid by 18 cycles of PCR amplification of the entire plasmid with the primers *WUSGUSPmF* and *WUSGUSPmR* (see Supplemental Table 2 online) that carry the mutated nucleotides using the Phusion DNA polymerase (Finnzymes). The resulting clones were sequenced to confirm the presence of the introduced mutations and the absence of unwanted mutations. The *WUS1.6*:*GUS*:*WUS3′wt* and *WUS1.6*:*GUS*:*WUS3′mut* plasmids were linearized by *Mlu*I digestion, and the inserts were recombined into *pEarleyGate303* (Earley et al., 2006) using a Gateway LR Clonase kit (Invitrogen) according to the manufacturer's instructions.

To construct *WUS3.2*:*GUS*:*WUS3′wt* and *WUS3.2*:*GUS*:*WUS3′mut*, the 3.2-kb *WUS* promoter was amplified by PCR using primers *WUS3.2proF* and *WUS3.2proR* (see Supplemental Table 2 online) and the plasmid *pIB39-WUS (HindIII-Bst1107I)*:*GUS* (a gift from T. Laux; Bäurle and Laux, 2005) as the template. The PCR product was cloned into *pGEM-T-easy* (Promega). The 3.2-kb promoter was released by *Not*I and *Sma*I digestion and cloned into *WUS1.6*:*GUS*:*WUS3′wt* or *WUS1.6*:*GUS*:*WUS3′mut* to replace the 1.6-kb promoter. The inserts in the *WUS3.2*:*GUS*:*WUS3′wt* and *WUS3.2*:*GUS*:*WUS3′mut* plasmids were then recombined into *pEarleyGate303* as described above.

In Situ Hybridization

In situ hybridization was performed as described (Chen et al., 2002). For the *WUS* probe, the *WUS* coding region was amplified by RT-PCR and cloned into pGEM-T-easy (Promega). This plasmid was digested with *Spe*I and transcribed with T7 RNA polymerase to generate the antisense probe. *STM* probe was prepared as described (Chuck et al., 1996). For generating the *GUS* probe, the PCR reaction was performed using

primers *GUST7* and *GUSSP6* (see Supplemental Table 2 online) and the *WUS1.6*:*GUS*:*WUS3′wt* plasmid as the template. In vitro transcription was performed with either T7 or SP6 RNA polymerase using the purified PCR product as the template to generate the antisense or sense probe, respectively.

Histochemical Staining

GUS staining was performed as described (Jefferson et al., 1987; Rodrigues-Pousada et al., 1993). Inflorescences were fixed in 90% cold acetone for 15 to 20 min and rinsed with the rinse solution [50 mM $NaPO_4$, pH 7.2, 0.5 mM $K_3Fe(CN)_6$, and 0.5 mM $K_4Fe(CN)_6$]. The infiltration solution [50 mM $NaPO_4$, pH 7.2, 0.5 mM $K_3Fe(CN)_6$, 0.5 mM $K_4Fe(CN)_6$, and 2 mM X-Gluc] was added, and the inflorescences were vacuum infiltrated for 10 min followed by incubation at 37°C overnight.

For Toluidine Blue staining, the tissue sections on slides were soaked in 0.1% Toluidine Blue in 0.1% sodium borate briefly and rinsed in water.

RNA Extraction and Gene Expression Analysis

The *35S*:*AG-GR ag-1* plants (Gómez-Mena et al., 2005; Sun et al., 2009) or *35S*:*AG-GR ag-1 clf-47* plants (generated in this study) were treated with DMSO, DEX (10 μM), CHX (10 μM), or DEX plus CHX (10 μM for each) in 0.015% Silwet L-77 by applying the solution onto inflorescences. At various time points after the chemical treatments, the inflorescences were dissected under a stereomicroscope to remove flowers of stage 9 or older, and RNA was isolated with TRI reagent (MRC). Contaminating DNA was eliminated with DNaseI (New England Biolabs) treatment, and reverse transcription was performed using M-MLV reverse transcriptase (Promega). Quantitative real-time RT-PCR was conducted in triplicate on the Bio-Rad IQ5 real-time PCR system using the SYBR Green PCR master mix (Applied Biosystems). Four to five biological replicates were conducted, and the results were analyzed with SPSS statistics 17.0 (IBM) using the independent-samples *t* test.

ChIP

ChIP was performed as described previously (Sun et al., 2009; Zheng et al., 2009) with slight modifications. Inflorescences were ground in liquid nitrogen and cross-linked with 1% formaldehyde in M1 buffer (10 mM phosphate buffer, pH 7.0, 0.1 M NaCl, 10 mM mercaptoethanol, 1 M hexylene glycol, 1× protease inhibitor cocktail [Roche], and 1 mM PMSF) for 10 min. The suspension was filtered through four layers of Miracloth, and the filtrate was centrifuged at 12,000 rpm for 10 min. The pelleted chromatin was washed three times with M2 buffer (M1 buffer plus 10 mM $MgCl_2$ and 0.5% Triton X-100) and once with M3 buffer (10 mM phosphate buffer, pH 7.0, 0.1 M NaCl, 10 mM mercaptoethanol, 1× protease inhibitor cocktail [Roche], and 1 mM PMSF). Chromatin was resuspended in nuclei lysis buffer and sonicated to generate DNA fragments of ~500 bp. The lysate was precleared by incubation with 50 μL protein-A agarose beads/salmon sperm DNA (Millipore) for 1 h and incubated with anti-HA (abcam), anti-H3K27me3 (abcam), or anti-AG antibodies (see below) overnight. The bound DNA fragments were recovered and purified with columns from the Plasmid Extraction kit (Qiagen) according to the manufacturer's instructions. Quantitative real-time PCR was performed on bound and input DNAs. Primers used are listed in Supplemental Table 2 online. AG antibodies were produced in rabbits against an AG-specific peptide at Sigma-Genosys. The antisera were purified using a C-terminal portion of AG protein expressed in *Escherichia coli* as a fusion to maltose binding protein.

For testing TFL2 occupancy at *WUS* by ChIP, entire inflorescences of Col (a negative control) and *35S*:*TFL2-3HA* were used. For testing AG binding to *WUS* by ChIP, entire inflorescences from L*er* and *ag-1* (a negative control) were used. For ChIP to examine the status of H3K27me3 in L*er* and *ag-1* or TFL2/LHP1 occupancy at *WUS* in *35S*:*TFL2-3HA* and *35S*:*TFL2-3HA ag-1*, microdissected inflorescences containing flowers of stage 8 and younger were used.

Laser Capture Microdissection

Laser capture microdissection was performed as described (http://seedgenenetwork.net/arabidopsis#procedure; Cai and Lashbrook, 2006; Hsieh et al., 2011) using the Arcturus laser capture microdissection instrument (Applied Biosystems). In brief, inflorescences from L*er* and *ag-1* plants were fixed with ethanol/acetic acid, dehydrated, and embedded in paraffin blocks. Ribbons with 8-μm sections were loaded on a slide and deparaffinized. Floral meristems at stages 1 and 2, 3, 4 and 5, and 6 were identified. A circular area covering the center of a meristem was excised from all the serial sections that contained that meristem. This ensured that all cells from the central region of an entire floral meristem were included. Total RNA was extracted with the Arcturus Picopure RNA isolation kit (Applied Biosystems) according to the manufacturer's protocol. Reverse transcription was conducted with M-MLV reverse transcriptase (Promega). Quantitative RT-PCR was performed in triplicate on the Bio-Rad IQ5 Real-time PCR system usingSYBR Green PCR master mix (Applied Biosystems). Two biological replicates were conducted.

Immunoblotting

One hundred milligrams of leaves or inflorescences from L*er* or *ag-10 clf-47* plants were ground in liquid nitrogen and homogenized in 2× SDS sample buffer (0.5 M Tris-HCl, pH 6.8, 4.4% [w/v] SDS, 20% [v/v] glycerol, 2% [v/v] 2-mercaptoethanol, and bromophenol blue). The samples were boiled for 10 min, cooled on ice for 5 min, and centrifuged at 16,000*g* for 5 min at 4°C to precipitate insoluble material. Proteins in the supernatant were resolved in a 12% SDS-PAGE gel, transferred to a nitrocellulose membrane, and probed with anti-AG antibodies. Signal development was performed with the ECL+Plus Western Blotting system (GE Healthcare) and by exposure of the membrane to x-ray film (Denville) at a time course of 30 s, 1 min, and 2 min. The time course ensured that the signal detection was within linear range.

Accession Numbers

Sequence data from this article can be found in the Arabidopsis Genome Initiative or GenBank/EMBL databases under the following accession numbers: *AG*, AT4G18960; *APETALA1*, AT1G69120; *APETALA3*, AT3G54340; *CLF*, AT2G23380; *eIF4A1*, AT3G13920; *KNU*, AT5G14010; *SPOROCYTELESS*, AT4G27330; *UBQ5*, AT3G62250; and *WUS*, AT2G17950.

Supplemental Data

The following materials are available in the online version of this article.

Supplemental Figure 1. Structure of the *CLF* Gene and Similarity between CLF and Other Eukaryotic E(z) Homologs within the SET Domain.

Supplemental Figure 2. Effects of the *clf-47* Mutation on *AG* Expression.

Supplemental Figure 3. *CLF* and *SWN* Are Responsible for H3K27 Trimethylation at the *WUS* Locus in Seedlings.

Supplemental Figure 4. A Time-Course Analysis of Gene Expression in Response to AG Induction in *35S*:*AG-GR ag-1* Inflorescences.

Supplemental Figure 5. GUS Staining and in Situ Hybridization to Examine *GUS* Expression in *WUS1.6*:*GUS*:*WUS3′mut* Transgenic Lines.

Supplemental Figure 6. Laser Capture Microdissection of Floral Meristems.

Supplemental Table 1. Floral Organ Counts in Flowers of Various Genotypes.

Supplemental Table 2. Oligonucleotides Used in This Study.

ACKNOWLEDGMENTS

We thank John Harada for valuable advice and protocols on laser capture microdissection. We thank Toshiro Ito, Thomas Laux, Robert Sablowski, Wenhui Shen, and Hao Yu for sharing materials and Yuanyuan Zhao and Thanh Theresa Dinh for comments on the manuscript. This work was supported by a grant from National Institutes of Health (GM61146) to X.C. R.M. and J.G. were funded by a grant from the UK Biotechnology and Biological Science Research Council. R.E.Y. was supported by a National Science Foundation Integrative Graduate Education and Research Traineeship training grant (DGE0504249). C.L. was supported by the National Natural Science Foundation of China (Grant 90919033) and the Chinese Academy of Sciences (Grant KSCX2-EW-Q-24-02).

AUTHOR CONTRIBUTIONS

X.L., Y.J.K., J.G., and X. Chen designed the research. X.L., Y.J.K., R.M., R.E.Y., C.L., and Y.P. performed research. C.L. and X. Cao contributed new analytic tools. X.L., Y.J.K., R.M., R.E.Y., Y.P., J.G., and X. Chen analyzed data. X. Chen, X.L., and Y.J.K. wrote the article.

Received September 10, 2011; revised October 6, 2011; accepted October 15, 2011; published October 25, 2011.

REFERENCES

Alvarez, J., and Smyth, D.R. (1999). *CRABS CLAW* and *SPATULA*, two *Arabidopsis* genes that control carpel development in parallel with *AGAMOUS.* Development **126:** 2377–2386.

Bäurle, I., and Laux, T. (2005). Regulation of *WUSCHEL* transcription in the stem cell niche of the *Arabidopsis* shoot meristem. Plant Cell **17:** 2271–2280.

Bowman, J.L., Sakai, H., Jack, T., Weigel, D., Mayer, U., and Meyerowitz, E.M. (1992). *SUPERMAN*, a regulator of floral homeotic genes in *Arabidopsis.* Development **114:** 599–615.

Bowman, J.L., Smyth, D.R., and Meyerowitz, E.M. (1989). Genes directing flower development in *Arabidopsis.* Plant Cell **1:** 37–52.

Boyer, L.A., et al. (2006). Polycomb complexes repress developmental regulators in murine embryonic stem cells. Nature **441:** 349–353.

Cai, S., and Lashbrook, C.C. (2006). Laser capture microdissection of plant cells from tape-transferred paraffin sections promotes recovery of structurally intact RNA for global gene profiling. Plant J. **48:** 628–637.

Carles, C.C., Choffnes-Inada, D., Reville, K., Lertpiriyapong, K., and Fletcher, J.C. (2005). *ULTRAPETALA1* encodes a SAND domain putative transcriptional regulator that controls shoot and floral meristem activity in *Arabidopsis.* Development **132:** 897–911.

Chanvivattana, Y., Bishopp, A., Schubert, D., Stock, C., Moon, Y.H., Sung, Z.R., and Goodrich, J. (2004). Interaction of Polycomb-group proteins controlling flowering in *Arabidopsis.* Development **131:** 5263–5276.

Chen, X., Liu, J., Cheng, Y., and Jia, D. (2002). *HEN1* functions pleiotropically in *Arabidopsis* development and acts in C function in the flower. Development **129:** 1085–1094.

Chuck, G., Lincoln, C., and Hake, S. (1996). *KNAT1* induces lobed leaves with ectopic meristems when overexpressed in *Arabidopsis.* Plant Cell **8:** 1277–1289.

Clark, S.E., Jacobsen, S.E., Levin, J.Z., and Meyerowitz, E.M. (1996). The CLAVATA and *SHOOT MERISTEMLESS* loci competitively regulate meristem activity in *Arabidopsis.* Development **122:** 1567–1575.

Das, P., Ito, T., Wellmer, F., Vernoux, T., Dedieu, A., Traas, J., and Meyerowitz, E.M. (2009). Floral stem cell termination involves the direct regulation of *AGAMOUS* by *PERIANTHIA.* Development **136:** 1605–1611.

Drews, G.N., Bowman, J.L., and Meyerowitz, E.M. (1991). Negative regulation of the *Arabidopsis* homeotic gene *AGAMOUS* by the *APETALA2* product. Cell **65:** 991–1002.

Earley, K.W., Haag, J.R., Pontes, O., Opper, K., Juehne, T., Song, K., and Pikaard, C.S. (2006). Gateway-compatible vectors for plant functional genomics and proteomics. Plant J. **45:** 616–629.

Gómez-Mena, C., de Folter, S., Costa, M.M., Angenent, G.C., and Sablowski, R. (2005). Transcriptional program controlled by the floral homeotic gene *AGAMOUS* during early organogenesis. Development **132:** 429–438.

Goodrich, J., Puangsomlee, P., Martin, M., Long, D., Meyerowitz, E.M., and Coupland, G. (1997). A Polycomb-group gene regulates homeotic gene expression in *Arabidopsis.* Nature **386:** 44–51.

Grossniklaus, U., Vielle-Calzada, J.P., Hoeppner, M.A., and Gagliano, W.B. (1998). Maternal control of embryogenesis by *MEDEA*, a polycomb group gene in *Arabidopsis.* Science **280:** 446–450.

Hennig, L., and Derkacheva, M. (2009). Diversity of Polycomb group complexes in plants: Same rules, different players? Trends Genet. **25:** 414–423.

Heo, J.B., and Sung, S. (2011). Vernalization-mediated epigenetic silencing by a long intronic noncoding RNA. Science **331:** 76–79.

Hsieh, T.F., Shin, J., Uzawa, R., Silva, P., Cohen, S., Bauer, M.J., Hashimoto, M., Kirkbride, R.C., Harada, J.J., Zilberman, D., and Fischer, R.L. (2011). Regulation of imprinted gene expression in Arabidopsis endosperm. Proc. Natl. Acad. Sci. USA **108:** 1755–1762.

Huang, H., Mizukami, Y., Hu, Y., and Ma, H. (1993). Isolation and characterization of the binding sequences for the product of the *Arabidopsis* floral homeotic gene *AGAMOUS.* Nucleic Acids Res. **21:** 4769–4776.

Ito, T., Wellmer, F., Yu, H., Das, P., Ito, N., Alves-Ferreira, M., Riechmann, J.L., and Meyerowitz, E.M. (2004). The homeotic protein AGAMOUS controls microsporogenesis by regulation of SPOROCYTELESS. Nature **430:** 356–360.

Jefferson, R.A., Kavanagh, T.A., and Bevan, M.W. (1987). GUS fusions: Beta-glucuronidase as a sensitive and versatile gene fusion marker in higher plants. EMBO J. **6:** 3901–3907.

Ji, L., et al. (2011). ARGONAUTE10 and ARGONAUTE1 regulate the termination of floral stem cells through two microRNAs in Arabidopsis. PLoS Genet. **7:** e1001358.

Jürgens, G. (1985). A group of genes controlling the spatial expression of the bithorax complex in *Drosophila.* Nature **316:** 153–155.

Kanhere, A., et al. (2010). Short RNAs are transcribed from repressed polycomb target genes and interact with polycomb repressive complex-2. Mol. Cell **38:** 675–688.

Khalil, A.M., et al. (2009). Many human large intergenic noncoding RNAs associate with chromatin-modifying complexes and affect gene expression. Proc. Natl. Acad. Sci. USA **106:** 11667–11672.

Köhler, C., and Villar, C.B. (2008). Programming of gene expression by Polycomb group proteins. Trends Cell Biol. **18:** 236–243.

Kotake, T., Takada, S., Nakahigashi, K., Ohto, M., and Goto, K. (2003). *Arabidopsis TERMINAL FLOWER 2* gene encodes a heterochromatin protein 1 homolog and represses both *FLOWERING LOCUS T* to regulate flowering time and several floral homeotic genes. Plant Cell Physiol. **44:** 555–564.

Larsson, A.S., Landberg, K., and Meeks-Wagner, D.R. (1998). The *TERMINAL FLOWER2* (*TFL2*) gene controls the reproductive transition and meristem identity in *Arabidopsis thaliana.* Genetics **149:** 597–605.

Laux, T., Mayer, K.F., Berger, J., and Jürgens, G. (1996). The *WUSCHEL* gene is required for shoot and floral meristem integrity in *Arabidopsis.* Development **122:** 87–96.

Lenhard, M., Bohnert, A., Jürgens, G., and Laux, T. (2001). Termination of stem cell maintenance in *Arabidopsis* floral meristems by interactions between *WUSCHEL* and *AGAMOUS.* Cell **105:** 805–814.

Lewis, E.B. (1978). A gene complex controlling segmentation in *Drosophila.* Nature **276:** 565–570.

Liu, C., Xi, W., Shen, L., Tan, C., and Yu, H. (2009). Regulation of floral patterning by flowering time genes. Dev. Cell **16:** 711–722.

Lohmann, J.U., Hong, R.L., Hobe, M., Busch, M.A., Parcy, F., Simon, R., and Weigel, D. (2001). A molecular link between stem cell regulation and floral patterning in *Arabidopsis.* Cell **105:** 793–803.

Long, J.A., Moan, E.I., Medford, J.I., and Barton, M.K. (1996). A member of the KNOTTED class of homeodomain proteins encoded by the *STM* gene of *Arabidopsis.* Nature **379:** 66–69.

Maier, A.T., Stehling-Sun, S., Wollmann, H., Demar, M., Hong, R.L., Haubeiss, S., Weigel, D., and Lohmann, J.U. (2009). Dual roles of the bZIP transcription factor PERIANTHIA in the control of floral architecture and homeotic gene expression. Development **136:** 1613–1620.

Masui, S., Nakatake, Y., Toyooka, Y., Shimosato, D., Yagi, R., Takahashi, K., Okochi, H., Okuda, A., Matoba, R., Sharov, A.A., Ko, M.S., and Niwa, H. (2007). Pluripotency governed by *Sox2* via regulation of *Oct3/4* expression in mouse embryonic stem cells. Nat. Cell Biol. **9:** 625–635.

Mayer, K.F., Schoof, H., Haecker, A., Lenhard, M., Jürgens, G., and Laux, T. (1998). Role of *WUSCHEL* in regulating stem cell fate in the *Arabidopsis* shoot meristem. Cell **95:** 805–815.

Mitsui, K., Tokuzawa, Y., Itoh, H., Segawa, K., Murakami, M., Takahashi, K., Maruyama, M., Maeda, M., and Yamanaka, S. (2003). The homeoprotein Nanog is required for maintenance of pluripotency in mouse epiblast and ES cells. Cell **113:** 631–642.

Müller, J., and Verrijzer, P. (2009). Biochemical mechanisms of gene regulation by polycomb group protein complexes. Curr. Opin. Genet. Dev. **19:** 150–158.

Mylne, J.S., Barrett, L., Tessadori, F., Mesnage, S., Johnson, L., Bernatavichute, Y.V., Jacobsen, S.E., Fransz, P., and Dean, C. (2006). LHP1, the *Arabidopsis* homologue of HETEROCHROMATIN PROTEIN1, is required for epigenetic silencing of *FLC.* Proc. Natl. Acad. Sci. USA **103:** 5012–5017.

Nichols, J., Zevnik, B., Anastassiadis, K., Niwa, H., Klewe-Nebenius, D., Chambers, I., Schöler, H., and Smith, A. (1998). Formation of pluripotent stem cells in the mammalian embryo depends on the POU transcription factor Oct4. Cell **95:** 379–391.

Pasini, D., Bracken, A.P., Hansen, J.B., Capillo, M., and Helin, K. (2007). The polycomb group protein Suz12 is required for embryonic stem cell differentiation. Mol. Cell. Biol. **27:** 3769–3779.

Payne, T., Johnson, S.D., and Koltunow, A.M. (2004). *KNUCKLES* (*KNU*) encodes a C2H2 zinc-finger protein that regulates development of basal pattern elements of the *Arabidopsis* gynoecium. Development **131:** 3737–3749.

Pien, S., and Grossniklaus, U. (2007). Polycomb group and trithorax group proteins in *Arabidopsis.* Biochim. Biophys. Acta **1769:** 375–382.

Prunet, N., Morel, P., Thierry, A.M., Eshed, Y., Bowman, J.L., Negrutiu, I., and Trehin, C. (2008). *REBELOTE*, *SQUINT*, and *ULTRAPETALA1* function redundantly in the temporal regulation of floral meristem termination in *Arabidopsis thaliana.* Plant Cell **20:** 901–919.

Riechmann, J.L., Wang, M., and Meyerowitz, E.M. (1996). DNA-binding properties of *Arabidopsis* MADS domain homeotic proteins APETALA1, APETALA3, PISTILLATA and AGAMOUS. Nucleic Acids Res. **24:** 3134–3141.

Rinn, J.L., Kertesz, M., Wang, J.K., Squazzo, S.L., Xu, X., Brugmann, S.A., Goodnough, L.H., Helms, J.A., Farnham, P.J., Segal, E., and Chang, H.Y. (2007). Functional demarcation of active and silent chromatin domains in human *HOX* loci by noncoding RNAs. Cell **129:** 1311–1323.

Rodrigues-Pousada, R.A., De Rycke, R., Dedonder, A., Van Caeneghem, W., Engler, G., Van Montagu, M., and Van Der Straeten, D. (1993). The *Arabidopsis* 1-Aminocyclopropane-1-Carboxylate Synthase Gene 1 is expressed during early development. Plant Cell **5:** 897–911.

Schatlowski, N., Creasey, K., Goodrich, J., and Schubert, D. (2008). Keeping plants in shape: Polycomb-group genes and histone methylation. Semin. Cell Dev. Biol. **19:** 547–553.

Schubert, D., Primavesi, L., Bishopp, A., Roberts, G., Doonan, J., Jenuwein, T., and Goodrich, J. (2006). Silencing by plant Polycomb-group genes requires dispersed trimethylation of histone H3 at lysine 27. EMBO J. **25:** 4638–4649.

Schultz, E.A., Pickett, F.B., and Haughn, G.W. (1991). The *FLO10* gene product regulates the expression domain of homeotic genes *AP3* and *PI* in *Arabidopsis* flowers. Plant Cell **3:** 1221–1237.

Shen, X., Liu, Y., Hsu, Y.J., Fujiwara, Y., Kim, J., Mao, X., Yuan, G.C., and Orkin, S.H. (2008). EZH1 mediates methylation on histone H3 lysine 27 and complements EZH2 in maintaining stem cell identity and executing pluripotency. Mol. Cell **32:** 491–502.

Shiraishi, H., Okada, K., and Shimura, Y. (1993). Nucleotide sequences recognized by the AGAMOUS MADS domain of *Arabidopsis thaliana in vitro.* Plant J. **4:** 385–398.

Smyth, D.R., Bowman, J.L., and Meyerowitz, E.M. (1990). Early flower development in *Arabidopsis.* Plant Cell **2:** 755–767.

Sun, B., Xu, Y., Ng, K.H., and Ito, T. (2009). A timing mechanism for stem cell maintenance and differentiation in the *Arabidopsis* floral meristem. Genes Dev. **23:** 1791–1804.

Sung, S., He, Y., Eshoo, T.W., Tamada, Y., Johnson, L., Nakahigashi, K., Goto, K., Jacobsen, S.E., and Amasino, R.M. (2006). Epigenetic maintenance of the vernalized state in *Arabidopsis thaliana* requires LIKE HETEROCHROMATIN PROTEIN 1. Nat. Genet. **38:** 706–710.

Tsai, M.C., Manor, O., Wan, Y., Mosammaparast, N., Wang, J.K., Lan, F., Shi, Y., Segal, E., and Chang, H.Y. (2010). Long noncoding RNA as modular scaffold of histone modification complexes. Science **329:** 689–693.

Turck, F., Roudier, F., Farrona, S., Martin-Magniette, M.L., Guillaume, E., Buisine, N., Gagnot, S., Martienssen, R.A., Coupland, G., and Colot, V. (2007). *Arabidopsis* TFL2/LHP1 specifically associates with genes marked by trimethylation of histone H3 lysine 27. PLoS Genet. **3:** e86.

Xu, L., and Shen, W.H. (2008). Polycomb silencing of *KNOX* genes confines shoot stem cell niches in *Arabidopsis.* Curr. Biol. **18:** 1966–1971.

Yap, K.L., Li, S., Muñoz-Cabello, A.M., Raguz, S., Zeng, L., Mujtaba, S., Gil, J., Walsh, M.J., and Zhou, M.M. (2010). Molecular interplay of the noncoding RNA *ANRIL* and methylated histone H3 lysine 27 by

polycomb CBX7 in transcriptional silencing of *INK4a.* Mol. Cell **38:** 662–674.

Zhang, X., Clarenz, O., Cokus, S., Bernatavichute, Y.V., Pellegrini, M., Goodrich, J., and Jacobsen, S.E. (2007b). Whole-genome analysis of histone H3 lysine 27 trimethylation in *Arabidopsis.* PLoS Biol. **5:** e129.

Zhang, X., Germann, S., Blus, B.J., Khorasanizadeh, S., Gaudin, V., and Jacobsen, S.E. (2007a). The *Arabidopsis* LHP1 protein colocalizes with histone H3 Lys27 trimethylation. Nat. Struct. Mol. Biol. **14:** 869–871.

Zhao, J., Sun, B.K., Erwin, J.A., Song, J.J., and Lee, J.T. (2008). Polycomb proteins targeted by a short repeat RNA to the mouse X chromosome. Science **322:** 750–756.

Zheng, B., and Chen, X. (2011). Dynamics of histone H3 lysine 27 trimethylation in plant development. Curr. Opin. Plant Biol. **14:** 123–129.

Zheng, B., Wang, Z., Li, S., Yu, B., Liu, J.Y., and Chen, X. (2009). Intergenic transcription by RNA polymerase II coordinates Pol IV and Pol V in siRNA-directed transcriptional gene silencing in *Arabidopsis.* Genes Dev. **23:** 2850–2860.